Proton entry into the near-lunar plasma wake for magnetic field aligned flow

M. B. Dhanya,[1] A. Bhardwaj,[1] Y. Futaana,[2] S. Fatemi,[2,3] M. Holmström,[2] S. Barabash,[2] M. Wieser,[2] P. Wurz,[4] A. Alok,[1] and R. S. Thampi[1]

[1]   We report the first observation of protons in the near-lunar (100–200 km from the surface) and deeper (near anti-subsolar point) plasma wake when the interplanetary magnetic field (IMF) and solar wind velocity (v_{sw}) are parallel (aligned flow; angle between IMF and $v_{sw} \leq 10°$). More than 98% of the observations during aligned flow condition showed the presence of protons in the wake. These observations are obtained by the Solar Wind Monitor sensor of the Sub-keV Atom Reflecting Analyser experiment on Chandrayaan-1. The observation cannot be explained by the conventional fluid models for aligned flow. Back tracing of the observed protons suggests that their source is the solar wind. The larger gyroradii of the wake protons compared to that of solar wind suggest that they were part of the tail of the solar wind velocity distribution function. Such protons could enter the wake due to their large gyroradii even when the flow is aligned to IMF. However, the wake boundary electric field may also play a role in the entry of the protons into the wake. **Citation:** Dhanya, M. B., A. Bhardwaj, Y. Futaana, S. Fatemi, M. Holmström, S. Barabash, M. Wieser, P. Wurz, A. Alok, and R. S. Thampi (2013), Proton entry into the near-lunar plasma wake for magnetic field aligned flow, *Geophys. Res. Lett.*, *40*, 2913–2917, doi:10.1002/grl.50617.

1. Introduction

[2]   The characteristics of lunar plasma wake at distances in the range of a fraction of lunar radius (near-lunar wake) to few lunar radii (far-lunar wake) are an evolving problem. The limited observations and simulations performed for the far-lunar wake have shown that the geometry of the wake depends on the orientation of the interplanetary magnetic field (IMF) [*Ogilvie et al.*, 1996; *Birch and Chapman*, 2002; *Trávníček et al.*, 2005; *Kallio*, 2005; *Wiehle et al.*, 2011; *Fatemi et al.*, 2013]. In the near-lunar wake, protons have been observed to enter the wake along IMF [*Futaana et al.*, 2010], as well as perpendicular to IMF [*Nishino et al.*, 2009a, 2009b; *Wang et al.*, 2010], when the IMF is predominantly perpendicular to the solar wind velocity. The entry

perpendicular to IMF requires either the convective electric field of solar wind [*Nishino et al.*, 2009b; *Wang et al.*, 2010] or an ambipolar potential drop across the wake boundary [*Nishino et al.*, 2009a] to assist the entry of protons into the wake. The situation when the solar wind velocity vector is aligned to the IMF (aligned flow) is a special case where none of the above mechanisms can transport protons to deeper locations inside the near-lunar wake. Recent [*Holmström et al.*, 2012] and past simulations [*Michel*, 1968; *Wolf*, 1968; *Spreiter et al.*, 1970] for the far-lunar wake have shown that the entry of solar wind protons to the near-lunar wake will be inhibited during aligned flow. However, one can expect solar wind proton entry due to their own gyromotion (provided that the gyroradius is larger) even under parallel IMF, but no observations have been reported. We report the unique events under weak IMF and high proton temperature that make the gyroradius larger and thus enable solar wind protons to enter the deeper wake. These first observations of protons in the near-lunar (100–200 km altitude) and deeper (closer to the antisubsolar point; about 45° and 61° from the terminator) wake during aligned flow have been made by the Solar Wind Monitor (SWIM)/Sub-keV Atom Reflecting Analyser (SARA) experiment aboard Chandrayaan-1.

2. Instrument and Data

[3]   The SWIM (Solar Wind Monitor) was an ion mass analyzer and was one of the two sensors of the SARA (Sub-keV Atom Reflecting Analyser) experiment on the 100–200 km polar-orbiting lunar spacecraft Chandrayaan-1 [*Bhardwaj et al.*, 2005; *Barabash et al.*, 2009; *McCann et al.*, 2007]. The other sensor, the Chandrayaan-1 Energetic Neutrals Analyzer, which was a neutral particle sensor, has observed energetic neutral hydrogen atoms in the near-lunar environment [*Wieser et al.*, 2009; *Futaana et al.*, 2012; *Bhardwaj et al.*, 2012; *Vorburger et al.*, 2012]. SWIM has a fan-shaped field of view (FOV) having 16 angular pixels with an angular resolution around $10° \times 4.5°$ (see Figure 1a for illustration). The FOV orientation changes from the pole to the equator such that the FOV plane is perpendicular to the ecliptic plane at the poles and parallel to the ecliptic plane at the equator, as illustrated in Figures 1b and 1c for two orbits when the orbital plane makes angles of 61° and 45°, respectively, with the day-night terminator plane. SWIM was operated in the energy range 100–3000 eV with an energy resolution of $\Delta E/E \sim 7\%$. The SWIM observations provide differential flux of ions in a specific energy and angular (direction) bin every 31.25 ms. The time taken for a full angular and energy scan was 8 s. Only the observations made when the Moon was located in the upstream solar

[1]Space Physics Laboratory, Vikram Sarabhai Space Centre, Thiruvananthapuram, India.
[2]Swedish Institute of Space Physics, Kiruna, Sweden.
[3]Department of Computer Science, Electrical and Space Engineering, Luleå University of Technology, Luleå, Sweden.
[4]Physikalisches Institut, University of Bern, Bern, Switzerland.

Corresponding author: M. B. Dhanya, Space Physics Laboratory, Vikram Sarabhai Space Centre, Thiruvananthapuram 695022, India. (dhanya_m_b@yahoo.co.in)
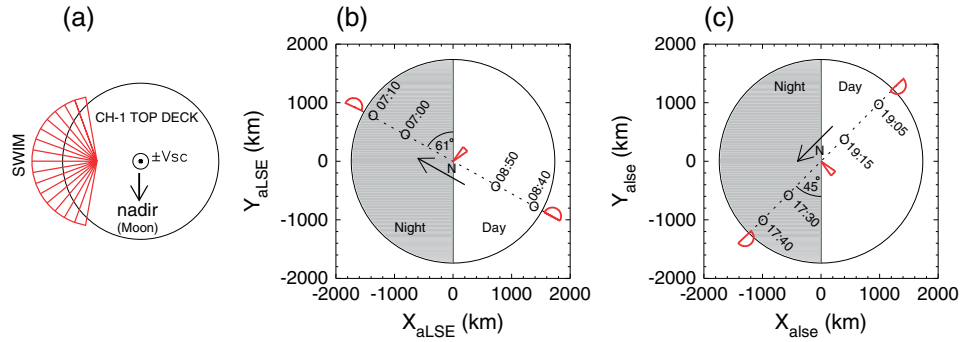
Figure 1. (a) Field of view (FOV) of SWIM mounted on the top deck of Chandrayaan-1. The direction of nadir and the velocity vector of the spacecraft (v_{sc}) are shown. (b) SWIM FOV orientation (shown in red) as seen from the lunar north pole (indicated as "N") for an orbit (dotted line) on 18 July 2009 between 07:00 UT and 08:50 UT. The angle between the orbital plane of Chandrayaan-1 and the day-night terminator plane (Sun aspect angle (SAA)) was 61°. The SWIM FOV plane is perpendicular to the ecliptic plane at the poles and is in the ecliptic plane closer to the equator. The nightside is shown by the grey-shaded area. The arrow indicates the direction of the motion of the spacecraft. (c) Same as Figure 1b but for 30 April 2009 (between 17:30 UT and 19:15 UT) when the Sun aspect angle was 45°.

wind (outside the Earth's bow shock) have been considered in the present analysis. The coordinate system used for the analysis is "aberrated Lunar-centric Solar Ecliptic (aLSE) coordinates," where the x axis is along the anti-solar wind velocity direction, the z axis is normal to the solar wind velocity vector toward the ecliptic north, and the y axis completes the right-handed coordinate system. For the upstream solar wind parameters, such as solar wind velocity, density, and IMF orientation, we have used level-2 data from the Solar Wind Electron, Proton, and Alpha Monitor and Magnetometer instruments on the ACE satellite. Since ACE makes measurements near the L1 point, the data have been time shifted by considering the solar wind speed and distance of ACE from the Moon. For the analysis in this paper, we considered the flow to be aligned when the angle between the solar wind velocity and IMF was within ±10°.

3. Observations

[4] The energy-time spectrogram of the proton counts observed by SWIM at 200 km altitude above the lunar surface on 18 July 2009, when the orbital plane of Chandrayaan-1 was at an angle of 61° from the day-night terminator, is shown in Figure 2a. The two populations of protons observed in this orbit are marked as A and B in Figure 2a. Our emphasis here is on population A observed in the wake when the solar zenith angle (SZA) was close to 140°. The orientation of IMF (Figure 2a, bottom) was aligned with the solar wind velocity within ±5°. The configuration of the SWIM field of view during this orbit is shown in Figure 1b. Hereafter, we refer to this observation as Event-1. Population B corresponds to upstream solar wind protons observed on the lunar dayside.

[5] Two events observed on 30 April 2009, in two consecutive orbits, are shown in Figure 2b, when the orbital plane of Chandrayaan-1 was at an angle of 45° from the day-night terminator and at an altitude of 100 km. For the orbit which spans 17:20–19:20 UT, intense proton counts were observed in the wake around 17:35–17:55 UT (indicated as A) when the SZA was close to 130°. The IMF was within ±10° of the solar wind velocity vector. We refer to

this observation as Event-2. Similarly, in the following orbit, proton counts are observed during 19:35–19:55 UT in the wake (indicated as A), when the IMF and solar wind velocity were aligned (within ±5°). Figure 1c shows the FOV orientation of SWIM for these orbits. We refer to this observation as Event-3. The summary of the three events along with the upstream solar wind parameters is given in Table 1.

[6] Over the 6 months (January–July 2009) of SWIM observations, the condition for the aligned flow (the angle between the solar wind and the IMF is less than 10°) was satisfied on 30 days in 66 orbits when SWIM was in the wake (the total number of SWIM data points was 3648). More than 98% of the observations in the lunar wake registered nonzero counts when the aligned flow condition was satisfied. In the analysis, counts = 1 (in every energy and direction bin) was considered as background and was subtracted from the observed counts.

4. Discussion

[7] For a perfect magnetic field aligned flow, the convective electric field ($\mathbf{E}_{conv}$) is zero. For an angle of ≤10° between the IMF and solar wind velocity, the convective electric field would be negligible. Hence, the transport of solar wind protons scattered on the dayside to the nightside under the influence of $\mathbf{E}_{conv} \times \mathbf{B}_{IMF}$ (gyroradius larger than the Moon radius, e.g., *Nishino et al.* [2009b]) would not be efficient for an aligned flow. Since the solar wind velocity and IMF are parallel, the entry of protons parallel to IMF [e.g., *Futaana et al.*, 2010] also cannot explain the reported proton observations in the deep near-lunar wake. The fluid approximation for aligned flow [*Michel*, 1968; *Wolf*, 1968], as well as the continuum magnetohydrodynamic (MHD) approach [*Spreiter et al.*, 1970], cannot explain the observed protons because they are observed in the near-lunar and deeper wake. Classical theory [*Spreiter et al.*, 1970] and the recent hybrid simulations [*Holmström et al.*, 2012] show that the entry of solar wind protons is inhibited when the IMF is aligned with the solar wind flow, resulting in an elongated wake. However, models that emphasize on the far-lunar wake have limited applicability in the near-lunar wake because, in the
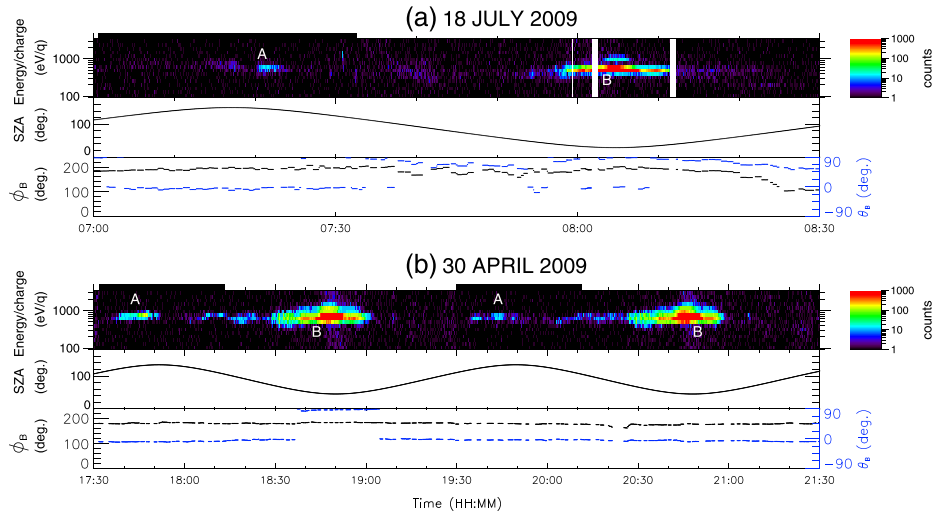
Figure 2. (a) SWIM observation on 18 July 2009 when the orbit of Chandrayaan-1 was at an altitude of 200 km. The top panel shows the energy-time spectrogram of proton counts with the black boxes overlaid representing the time interval when Chandrayaan-1 was in the lunar plasma wake. The population marked as A represents protons observed in the wake, and B represents upstream solar wind protons. The middle panel represents the solar zenith angle (SZA), and the bottom panel represents the orientation of IMF in terms of azimuth and elevation angles. The azimuth angle ϕ_B is the angle between the projection of IMF in the x-y plane and the x axis, whereas the elevation angle θ_B is the angle between the z component of IMF and the x-y plane, so that +90° refers to the orientation toward north and –90° refers to the orientation toward south (all in the aLSE frame). The orbit of Chandrayaan-1 for this event is shown in Figure 1b. (b) Same as Figure 2a but for 30 April 2009 when the orbit of Chandrayaan-1 was at an altitude of 100 km. The orbit of Chandrayaan-1 for this event is shown in Figure 1c.

near-lunar wake, the plasma dynamics is much more complicated due to the presence of processes such as lunar surface charging [*Halekas et al.*, 2011].

[8] The observed energy provides the speed of the protons and the viewing direction provides the direction of travel of the particle in the SWIM instrument frame. We have computed the velocity distribution of the observed protons in the aLSE frame, using full wake observations. For this, we have defined a spherical coordinate system (v, ϕ, θ) in the velocity space (see Figure 3a for illustration), where v is the velocity magnitude, ϕ is the velocity vector azimuth angle [0°, 360°], and θ is the velocity elevation angle [–90°, +90°]. The velocity distributions for Event-1 and Event-2 are shown in Figures 3b and 3c, respectively. It can be seen from Figure 3b that for Event-1, most of the protons observed by SWIM were traveling in the direction of ϕ of 210–260° and θ of +20 to –20°. The energy is around 700–800 eV. For Event-2, which happened on the dawnside hemisphere (whereas Event-1 was observed in the duskside hemisphere), SWIM has observed protons traveling mostly in the direction of ϕ of 120–180° and θ of 0° to +40°. Also, for this event, most of the observed protons have energy around 700 eV. According to the ACE data, the average energy of the solar wind was ∼420 eV for Event-1 (for an average

solar wind speed of 290 km s⁻¹; cf. Table 1) and ∼560 eV for Event-2 (for an average solar wind speed of 335 km s⁻¹; cf. Table 1). The angular velocity distribution of the protons for Event-3 was similar to that of Event-2 and therefore is not shown here.

[9] To understand the origin of the nightside ions, we back-traced the observed protons from the location of their detection using the observed velocity magnitude and direction. A similar method had been used, for example, by *Futaana et al.* [2003], for studying Moon-solar wind proton interaction. Here the back tracing was carried out with uniform (constant in time and position) upstream parameters as shown in Table 1. We assumed, for simplicity, that the magnetic field direction is perfectly parallel to the solar wind velocity vector. As an example, Figure 4 shows projections in two planes (x-y and x-z) of the back-traced trajectories of the observed protons during Event-2. These trajectories show that the majority of the observed protons could have originated from the solar wind. Some particles may come from the lunar surface, but the fraction is small. These solar wind ions could enter the wake due to their larger gyroradii even when the flow is aligned to IMF. The larger gyroradii of the wake protons compared with the solar wind gyroradii (∼95 km in the Event-2 case) suggest that they were part

Table 1. Summary of the Events and the Upstream Solar Wind Parameters[a]

Date	Event	SAA (°)	Time (UT)	SZA (°)	v_{sw} (km s⁻¹)	n_p (cm⁻³)	T_p (°K)	IMF (nT)
18 July 2009	Event-1	61	07:20–07:25	160–140	290	3	2×10^4	1
30 April 2009	Event-2	45	17:35–17:55	120–140	335	6	4.5×10^4	3
30 April 2009	Event-3	45	19:35–19:55	120–140	335	6	4.5×10^4	3

[a]SAA = Sun aspect angle, which is the angle between the orbital plane of Chandrayaan-1 and the day-night terminator plane; SZA = solar zenith angle; v_{sw} = solar wind speed (ACE); n_p = solar wind proton density (ACE); T_p = solar wind proton temperature (Wind); IMF = interplanetary magnetic field (ACE).
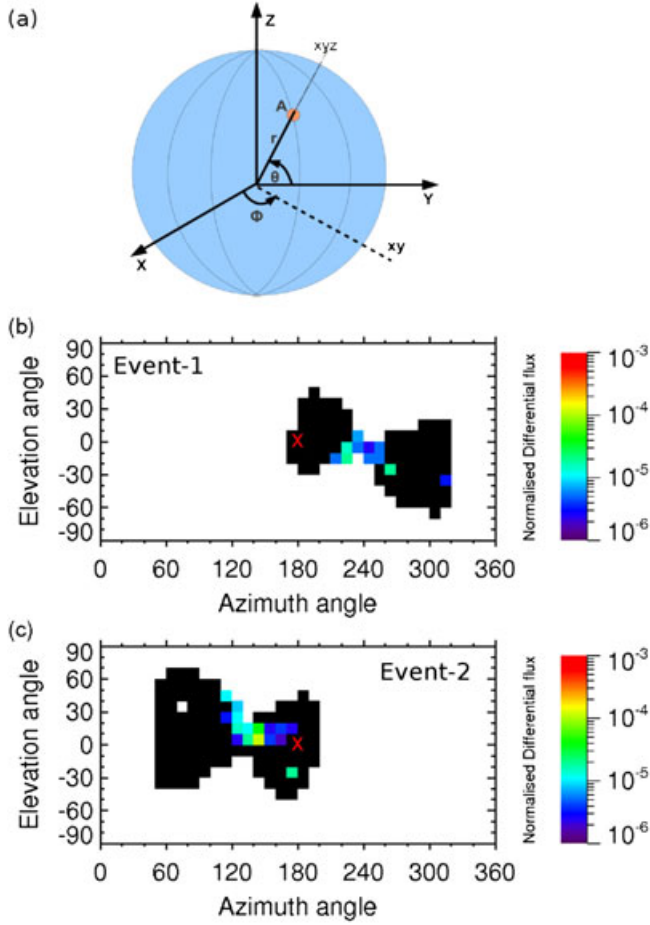
Figure 3. (a) The spherical polar coordinate system (origin at the center of the Moon) used to represent the velocity distribution of the wake protons, where ϕ is the velocity vector azimuth angle [0°, 360°] in the *x-y* plane and θ is the velocity elevation angle [–90°, +90°] as measured from the *z axis* of aLSE. The position "A" represents an arbitrary location of SWIM/Chandrayaan-1. (b) Velocity distribution of protons for Event-1, where the color bar represents the differential flux normalized to the solar wind flux (normalized differential flux). The black-filled areas represent zero counts observed by SWIM. The direction of solar wind (from ACE) is shown by the cross (red) symbol. (c) Same as Figure 3b but for Event-2.

[10] It should be noted that an ambipolar electric field formed at the boundary of the lunar wake [*Ogilvie et al.*, 1996; *Futaana et al.*, 2001] pointing inward can help the entry of solar wind protons into the wake. Thus, the observed cross-field entry of the solar wind protons may be a manifestation of the combination of thermal motion and wake boundary electric field.

[11] The presence of these protons, which were not expected in the near-lunar wake for an aligned flow, can alter the electrodynamics in the near-lunar wake region. The lunar surface charging on the nightside may also be affected due to these protons, which otherwise is negatively charged to potentials of around few hundred volts [*Halekas et al.*, 2011]. These protons, which possibly are from the high-energy tail of the solar wind, will cause sputtering when they hit the lunar nightside surface. According to *Wurz et al.* [2007], the total sputter yield per incident solar wind ion (mix of protons and alpha particles) typically is 0.1, for solar wind speed in the range 300–800 km s^{-1}, with a slight dependence on solar wind speed. For the various species present on the lunar surface, this sputter yield is modified by the abundance on the surface and is in the range 2×10^{-5} to 0.07 (the highest value being for oxygen). For an incident solar wind flux of $\sim 10^8$ cm^{-2} s^{-1}, we obtain a sputtered flux from the surface of about $\sim 10^7$ cm^{-2} s^{-1} corresponding to a total contribution to the exospheric density at the surface of up to 10 cm^{-3} [*Wurz et al.*, 2007]. Since, in our observation, the protons are observed mostly in three viewing directions of SWIM, the angular extension of the distribution is 30° × 30°. If we do a crude estimate of the flux of the protons for Event-1, we obtain a value around 1.1×10^6 cm^{-2} s^{-1}. If all

of the tail of the solar wind velocity distribution function. Only uniform electric and magnetic fields are assumed in the entire simulation domain. However, we examined the back tracing using an enhanced IMF magnitude (by a factor of 1.5 as an upper limit) to simulate the enhancement of the magnetic field in the wake [*Colburn et al.*, 1967; *Halekas et al.*, 2005]. The back tracing results were almost identical. We also examined small angles between the solar wind velocity and IMF in the range 5°–10°, and the results did not change significantly as well. This back tracing shows that the wake ions are likely of the solar wind origin. On the other hand, how much the solar wind can penetrate into the deep near-lunar wake is a further study. For that, the comparison with hybrid simulation would be a good tool [e.g., *Fatemi et al.*, 2012].
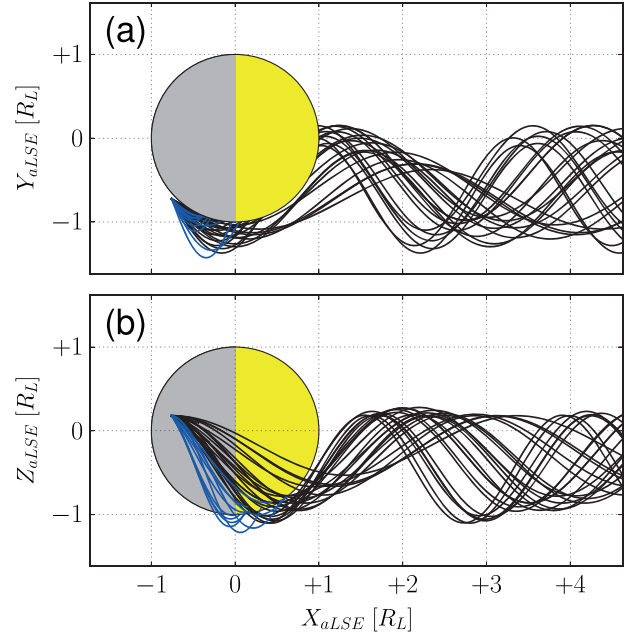

Figure 4. (a) Back-traced trajectories of the observed protons in Event-2 projected onto the *x-y* plane in the aLSE frame. The black curves show trajectories originating from the solar wind, and the blue curves show trajectories originating from the lunar surface. The unit of the horizontal and vertical axes is in lunar radii (R_L). (b) Same as Figure 4a but with trajectories projected onto the *x-z* plane.

these protons hit the nightside surface, we get a total contribution to the exospheric density at the surface of 0.1 cm^{-3}, based on the exosphere model by *Wurz et al.* [2007], which is dominated by oxygen but with a contribution of all the other species present on the lunar surface. This is only a crude upper limit for the contribution to the nightside exosphere from the wake protons since not all of the observed protons in the wake will hit the surface. For Event-2 and Event-3, the contributions to the exosphere are higher due to the higher differential flux of observed wake protons. Although this is only a crude estimate, it already indicates that the sputtered flux, and thus the contribution to the exosphere, will be very low. A detailed and more accurate estimation can be addressed in a future work. These results apply not only to the Moon but also to similar atmosphereless planetary bodies such as some of the satellites of the outer planets.

5. Conclusion

[12] We have reported observations of protons in the near-lunar (100–200 km from the lunar surface) and deeper (~45°–61° from the day-night terminator) wake during the aligned flow. These observations cannot be explained by the conventional fluid models for aligned flow. Back tracing of the observed protons suggests that their origin could be the solar wind. The computed larger gyroradii of the wake protons compared to that of solar wind imply that these must be from the tail of the solar wind velocity distribution. Such protons could indeed enter the wake even during aligned flow due to their larger gyroradii. However, the wake boundary electric field may assist the entry of the protons into the wake. These protons can alter the electrodynamics in the near-lunar wake region and may contribute toward the nightside exosphere by causing sputtering.

References

Barabash, S., et al. (2009), Investigation of the solar wind-Moon interaction onboard Chandrayaan-1 mission with the SARA experiment, *Curr. Sci.*, *96*(4), 526–532.

Bhardwaj, A., S. Barabash, Y. Futaana, Y. Kazama, K. Asamura, R. Sridharan, M. Holmström, P. Wurz, and R. Lundin (2005), Low energy neutral atom imaging on the Moon with the SARA instrument aboard Chandrayaan-1 mission, *J. Earth Syst. Sci.*, *114*(6), 749–760.

Bhardwaj, A., et al. (2012), Interaction of solar wind with Moon: An overview on the results from the SARA experiment aboard Chandrayaan-1, *Adv. Geosci.*, *30*, 35–55.

Birch, P. C., and S. C. Chapman (2002), Two dimensional particle-in-cell simulations of the lunar wake, *Phys. Plasmas*, *9*, 1785–1789.

Colburn, D. S., R. G. Currie, J. D. Mihalov, and C. P. Sonett (1967), Diamagnetic solar wind cavity 324 discovered behind the Moon, *Science*, *158*, 1040–1042.

Fatemi, S., M. Holmström, and Y. Futaana (2012), The effects of lunar surface plasma absorption and solar wind temperature anisotropies on the solar wind proton velocity space distributions in the low-altitude lunar plasma wake, *J. Geophys. Res.*, *117*, A10105, doi:10.1029/2011JA017353.

Fatemi, S., M. Holmström, Y. Futaana, S. Barabash, and C. Lue (2013), The lunar wake current systems, *Geophys. Res. Lett.*, *40*, 17–21, doi:10.1029/2012GL054635.

Futaana, Y., S. Machida, Y. Saito, A. Matsuoka, and H. Hayakawa (2001), Counterstreaming electrons in the near vicinity of the Moon observed by plasma instruments on board Nozomi, *J. Geophys. Res.*, *106*, 18,729–18,740.

Futaana, Y., S. Machida, Y. Saito, A. Matsuoka, and H. Hayakawa (2003), Moon-related nonthermal ions observed by Nozomi: Species, sources, and generation mechanisms, *J. Geophys. Res.*, *108*(A1), 1025, doi:10.1029/2002JA009366.

Futaana, Y., et al. (2010), Protons in the near-lunar wake observed by the Sub-keV Atom Reflection Analyzer on board Chandrayaan-1, *J. Geophys. Res.*, *115*, A10248, doi:10.1029/2010JA015264.

Futaana, Y., et al. (2012), Empirical energy spectra of neutralized solar wind protons from the lunar regolith, *J. Geophys. Res.*, *117*, E05005, doi:10.1029/2011JE004019.

Halekas, J. S., S. D. Bale, D. L. Mitchell, and R. P. Lin (2005), Electrons and magnetic fields in the lunar plasma wake, *J. Geophys. Res.*, *110*, A07222, doi:10.1029/2004JA010991.

Halekas, J. S., Y. Saito, G. T. Delory, and W. M. Farrell (2011), New views of the lunar plasma environment, *Planet. Space Sci*, *59*, 1681–1694, doi:10.1016/j.pss.2010.08.011.

Holmström, M., S. Fatemi, Y. Futaana, and H. Nilsson (2012), The interaction between the Moon and the solar wind, *Earth Planets Space*, *64*, 237–245.

Kallio, E. (2005), Formation of the lunar wake in quasi-neutral hybrid model, *Geophys. Res. Lett.*, *32*, L06107, doi:10.1029/2004GL021989.

McCann, D., S. Barabash, H. Nilsson, and A. Bhardwaj (2007), Miniature ion mass analyser, *Planet. Space Sci.*, *55*(9), 1190–1196, doi:10.1016/j.pss.2006.11.020.

Michel, F. C. (1968), Magnetic field structure behind the Moon, *J. Geophys. Res.*, *73*, 1533–1542.

Nishino, M. N., et al. (2009a), Pairwise energy gain-loss feature of solar wind protons in the near-Moon wake, *Geophys. Res. Lett.*, *36*, L12108, doi:10.1029/2009GL039049.

Nishino, M. N., et al. (2009b), Solar-wind proton access deep into the near-Moon wake, *Geophys. Res. Lett.*, *36*, L16103, doi:10.1029/2009GL039444.

Ogilvie, K. W., J. T. Steinberg, R. J. Fitzenreiter, C. J. Owen, A. J. Lazarus, W. M. Farrell, and R. B. Torbert (1996), Observations of the lunar plasma wake from the WIND spacecraft on December 27, 1994, *Geophys. Res. Lett.*, *10*, 1255–1258.

Spreiter, J. R., M. C. Marsch, and A. L. Summers (1970), Hydromagnetic aspects of solar wind flow past the Moon, *Cosmic Electrodynam.*, *1*, 5–50.

Trávníček, P., P. Hellinger, D. Schriver, and S. D. Bale (2005), Structure of the lunar wake: Two-dimensional global hybrid simulations, *Geophys. Res. Lett.*, *32*, L06102, doi:10.1029/2004GL022243.

Vorburger, A., P. Wurz, S. Barabash, M. Wieser, Y. Futaana, M. Holmström, A. Bhardwaj, and K. Asamura (2012), Energetic neutral atom observations of magnetic anomalies on the lunar surface, *J. Geophys. Res.*, *117*, A07208, doi:10.1029/2012JA017553.

Wang, X.-D., et al. (2010), Acceleration of scattered solar wind protons at the polar terminator of the Moon: Results from Chang'E-1/SWIDs, *Geophys. Res. Lett.*, *37*, L07203, doi:10.1029/2010GL042891.

Wiehle, S., et al. (2011), First lunar wake passage of ARTEMIS: Discrimination of wake effects and solar wind fluctuations by 3D hybrid simulations, *Planet. Space Sci.*, *59*(8), 661–671, doi:10.1016/j.pss.2011.01.012.

Wieser, M., et al. (2009), Extremely high reflection of solar wind protons as neutral hydrogen atoms from regolith in space, *Planet. Space Sci.*, *57*, 2132–2134, doi:10.1016/j.pss.2009.09.012.

Wolf, R. A. (1968), Solar-wind flow behind the Moon, *J. Geophys. Res.*, *73*, 4281–4289.

Wurz, P., U. Rohner, J. A. Whitby, C. Kolbb, H. Lammer, P. Dobnikar, and J. A. Martín-Fernández (2007), The lunar exosphere: The sputtering contribution, *Icarus*, *191*, 486–496.